How to cite: *Angew. Chem. Int. Ed.* **2022,** *61,* e202207137
International Edition: doi.org/10.1002/anie.202207137
German Edition: doi.org/10.1002/ange.202207137

NMR Spectroscopy

Magnesium(II)-ATP Complexes in 1-Ethyl-3-Methylimidazolium Acetate Solutions Characterized by ^{31}Mg β-Radiation-Detected NMR Spectroscopy

Ryan M. L. McFadden[+], Dániel Szunyogh[+], Nicholas Bravo-Frank, Aris Chatzichristos, Martin H. Dehn, Derek Fujimoto, Attila Jancsó, Silke Johannsen, Ildikó Kálomista, Victoria L. Karner, Robert F. Kiefl, Flemming H. Larsen, Jens Lassen, C. D. Philip Levy, Ruohong Li, Iain McKenzie, Hannah McPhee, Gerald D. Morris, Matthew R. Pearson, Stephan P. A. Sauer, Roland K. O. Sigel, Peter W. Thulstrup, W. Andrew MacFarlane, Lars Hemmingsen, and Monika Stachura**

Dedicated to Professor Paul Heitjans on the occasion of his 75th birthday

Abstract: The complexation of Mg^{II} with adenosine 5′-triphosphate (ATP) is omnipresent in biochemical energy conversion, but is difficult to interrogate directly. Here we use the spin-$^1/_2$ β-emitter ^{31}Mg to study Mg^{II}-ATP complexation in 1-ethyl-3-methylimidazolium acetate (EMIM-Ac) solutions using β-radiation-detected nuclear magnetic resonance (β-NMR). We demonstrate that (nuclear) spin-polarized ^{31}Mg, following ion-implantation from an accelerator beamline into EMIM-Ac, binds to ATP within its radioactive lifetime before depolarizing. The evolution of the spectra with solute concentration indicates that the implanted ^{31}Mg initially bind to the solvent acetate anions, whereafter they undergo dynamic exchange and form either a mono- (^{31}Mg-ATP) or di-nuclear (^{31}MgMg-ATP) complex. The chemical shift of ^{31}Mg-ATP is observed up-field of ^{31}MgMg-ATP, in accord with quantum chemical calculations. These observations constitute a crucial advance towards using β-NMR to probe chemistry and biochemistry in solution.

[*] Dr. R. M. L. McFadden,[+] Prof. Dr. R. F. Kiefl, Dr. J. Lassen, Dr. C. D. P. Levy, Dr. R. Li, Dr. I. McKenzie, Dr. G. D. Morris, Dr. M. R. Pearson, Prof. Dr. W. A. MacFarlane, Dr. M. Stachura
TRIUMF, 4004 Wesbrook Mall, Vancouver, BC V6T 2A3 (Canada)
E-mail: mstachura@triumf.ca

Dr. D. Szunyogh,[+] Dr. I. Kálomista, Prof. Dr. S. P. A. Sauer, Prof. Dr. P. W. Thulstrup, Prof. Dr. L. Hemmingsen
Department of Chemistry, University of Copenhagen, Universitetsparken 5, 2100 Copenhagen (Denmark)
E-mail: lhe@chem.ku.dk

N. Bravo-Frank
Faculty of Engineering, University of Victoria, 3800 Finnerty Road, Victoria, BC V8P 5C2 (Canada)

Dr. A. Chatzichristos, Dr. M. H. Dehn, Dr. D. Fujimoto, Prof. Dr. R. F. Kiefl, Prof. Dr. W. A. MacFarlane
Department of Physics and Astronomy, University of British Columbia, 6224 Agricultural Road, Vancouver, BC V6T 1Z1 (Canada)

Dr. A. Chatzichristos, Dr. M. H. Dehn, Dr. D. Fujimoto, Dr. V. L. Karner, Prof. Dr. R. F. Kiefl
Stewart Blusson Quantum Matter Institute, University of British Columbia, 2355 East Mall, Vancouver, BC V6T 1Z4 (Canada)

Prof. Dr. A. Jancsó
Department of Inorganic and Analytical Chemistry, University of Szeged, Dóm tér 7, 6720 Szeged (Hungary)

Dr. S. Johannsen, Prof. Dr. R. K. O. Sigel
Department of Chemistry, University of Zurich, Winterthurerstrasse 190, 8057 Zürich (Switzerland)

Dr. V. L. Karner, Prof. Dr. W. A. MacFarlane
Department of Chemistry, University of British Columbia 2036 Main Mall, Vancouver, BC V6T 1Z1 (Canada)

Prof. Dr. F. H. Larsen
Department of Food Science, University of Copenhagen, Roligheds-vej 26, 1958 Frederiksberg (Denmark)

Dr. J. Lassen
Department of Physics, Simon Fraser University, 8888 University Drive, Burnaby, BC V5A 1S6 (Canada)

Dr. J. Lassen
Department of Physics and Astronomy, University of Manitoba 30A Sifton Road, Winnipeg, MB R3T 2N2 (Canada)

Dr. I. McKenzie, Dr. M. Stachura
Department of Chemistry, Simon Fraser University, 8888 University Drive, Burnaby, BC V5A 1S6 (Canada)

Dr. I. McKenzie
Department of Physics and Astronomy, University of Waterloo, 200 University Avenue West, Waterloo, ON N2L 3G1 (Canada)

H. McPhee
Department of Engineering, McMaster University, 1280 Main Street West, Hamilton, ON L8S 4L7 (Canada)

[+] These authors contributed equally to this work.

Introduction

A key difficulty in elucidating the (bio)chemical function of Mg^{II} is the limited sensitivity of spectroscopic techniques capable of directly probing the closed shell ion.[1] Consequently, studies of its coordination chemistry are rather sparse (see e.g., ref. [2,3]), despite the physiological importance of Mg^{II}.[4] Having an experimental technique effective at resolving these details would greatly benefit all fields concerned with understanding the chemistry of Mg^{II}. While nuclear magnetic resonance (NMR) spectroscopy is used ubiquitously to this end for many elements, magnesium has only a single (stable) NMR isotope, ^{25}Mg (nuclear spin $I=5/2$; gyromagnetic ratio $\gamma/(2\pi)=-2.60793(9)\,MHz\,T^{-1}$; electric quadrupole moment $Q=199(2)\,mb$; 10 % natural abundance),[5,6] whose utility as a probe suffers from its non-zero quadrupole moment and low receptivity.[7,8] For example, the salient feature of Mg^{II} binding to a ligand such as adenosine 5′-triphosphate (ATP) is typically line broadening, obscuring fine structural signatures. To circumvent these limitations, we instead use the short-lived β-emitter ^{31}Mg (nuclear spin $I=1/2$; gyromagnetic ratio $\gamma/(2\pi)=-13.4699(23)\,MHz\,T^{-1}$; half-life $T_{1/2}=236\,ms$)[5,6,9] as our NMR probe and monitor its resonance through the anisotropic property of its β-decay—a technique known as β-radiation-detected NMR (β-NMR) spectroscopy.[10–12]

The principles of β-NMR are nearly identical to "conventional" NMR (see e.g., ref. [13]), with differences originating from the use of an unstable probe (e.g., NMR detected via radioactive decay products).[10–12] This approach affords a nearly $\approx 10^{10}$-fold increase in sensitivity, enabling spectra to be acquired under conditions which cannot be attained by any other method—including very low probe concentrations (see e.g., ref. [14–16]). In this sense, β-NMR is quite similar to muon spin spectroscopy (μSR).[17] While μSR is known for its utility in chemistry (see e.g.,[18]), β-NMR's uses are traditionally rooted in nuclear[19] and solid-state[11] physics, with chemical applications being relatively unexplored. Some progress to this end has been made recently,[12] with ^{8}Li β-NMR being used to study the glassy phase of polymers,[20–23] small molecules,[24] and room temperature ionic liquids (RTILs).[25] Similarly, several groups have now implemented setups capable of measurements in liquids,[16,26–31] greatly expanding the scope of possible experiments.[32]

Our primary interest here is applying ^{31}Mg β-NMR to study Mg^{II} complexation in solution.[33] Distinct from "conventional" NMR, nuclear spin polarized ^{31}Mg is introduced into solution by ion-implantation in an accelerator beamline under ultra-high vacuum (UHV).[16,34] A question that naturally arises is: does ^{31}Mg, following implantation, attain an equilibrium configuration within its radioactive lifetime? This is indeed the case when the solvent molecules are the ligands in the coordination complex that forms, as was demonstrated in two imidazolium based RTILs.[16] With the current work, we aim to progress to the more interesting situation of ^{31}Mg binding to a foreign solute molecule. To this end, we implanted ^{31}Mg into a series of 1-ethyl-3-methylimidazolium acetate (EMIM-Ac) solutions containing the prototypical Mg^{II} ligand in biochemistry, ATP. *A priori*, it was not obvious if the probe would associate with the biomolecule both within its radioactive lifetime and before its spin polarization was lost (via spin-lattice relaxation). As we shall show below, both of these conditions are fulfilled.

The Mg^{II}-ATP complex was selected due to its ubiquitous function in biochemistry as an "energy currency".[35,36] For example, Mg^{II}-catalyzed ATP hydrolysis within enzymes is coupled directly to, and drives otherwise non-spontaneous, biochemical processes. Moreover, though the RTIL solvent is quite different from an aqueous medium, it provides a coordination environment akin to Mg^{II} binding in proteins;[37,38] the abundant acetate ligands (≈ 6 M) resemble both glutamate and aspartate side chains, while EMIM-Ac's dielectric constant[39] is compatible with the range of values commonly reported for the interior of proteins (see e.g., ref. [38]). Thus, both electrostatically and in terms of ligand composition, EMIM-Ac resembles Mg^{II}-ATP binding sites in enzymes both within ATP hydrolysis and in phosphoryl transfer, though lacking specific optimized structures typically present in proteins.

Results and Discussion

Before discussing the observed ^{31}Mg β-NMR spectra, we digress briefly into the most essential experimental details. In these β-NMR experiments,[40] performed at TRIUMF's isotope separator and accelerator (ISAC) facility, ^{31}Mg was extracted from an isotope production target (as a 40 keV $^{31}Mg^{I}$ beam) by laser ionization, spin-polarized in-flight by optical pumping,[41,42] and implanted into the EMIM-Ac solution. The solution, housed in an aluminum alloy holder, was suspended vertically in UHV (10^{-10} Torr), where EMIM-Ac's virtually zero vapour pressure prevented evaporation,[16,25,43] and its large viscosity (see e.g., ref. [44]) inhibited flow out of the container.[16,25] During implantation, the probe rapidly oxidizes to $^{31}Mg^{II}$,[16] and its ensuing behaviour reflects the chemical properties of the closed shell ion. The β NMR measurements were performed at 295 K and 3.20 T (corresponding to a Larmor frequency of ≈ 43.1 MHz for ^{31}Mg) using a dedicated high-field spectrometer.[11,45] Resonances were acquired using a continuous wave (CW) radio frequency (RF) transverse magnetic field B_1 that was slowly stepped through ^{31}Mg's Larmor frequency, integrating for 1 s at each frequency step. This approach is analogous to a CW NMR experiment[46] using stable nuclei and similar to the approach adopted in μSR.[47] Off resonance (or in absence of any RF field), the β-decay asymmetry (proportional to the spin-polarization of the ^{31}Mg ensemble[40]) is constant, with this "baseline" value setting the maximum possible signal amplitude (see e.g., ref. [11]). On resonance, the ^{31}Mg nuclei are rapidly depolarized, resulting in a reduction in the observed asymmetry, with a value of ≈ 0 corresponding to the complete ^{31}Mg population visiting a particular "site" (i.e., coordination environment) during the measurement time window; however, if exchange dynamics occur (i.e., the probes occupy more than one structure within the duration of the RF

pulse), they can contribute to each resonance peak, giving rise to double-counting. We observe this "extra" amplitude in all spectra, highlighting the importance of chemical exchange in our measurements.

Prior to embarking on the β-NMR measurements, it was important to first confirm the complexation of Mg^{II} and ATP in EMIM-Ac. For this, we applied ^{31}P NMR spectroscopy to explore the equilibrium chemistry of the binding process.[40] These measurements established that Mg^{II} binds to ATP under our experimental conditions, allowing for estimates of equilibrium constants for the formation of Mg-ATP and Mg_2-ATP.[40] Next, ^{31}Mg β-NMR experiments were conducted (see Figure 1), as outlined below.

First, a ^{31}Mg β-NMR spectrum was recorded with 25 mM $MgCl_2$ (anhydrous) dissolved in EMIM-Ac, but in the absence of ATP (i.e., representing Mg^{II} binding to the solvent acetate anions). Note that without the added salt, the spectrum is broad with poorly resolved features;[16] however, with the impurity sites saturated by stable "carrier" Mg^{II}, the spectra sharpen, revealing two characteristic "solvent" peaks. Further increasing the $MgCl_2$ concentration had little effect on the signal.[40] The most consequential feature of the "solvent" signal is the large amplitude peak, which is easily identified in all spectra and we assign it a chemical shift of 0 ppm, making it our in situ reference for the ^{31}Mg spectra.[40]

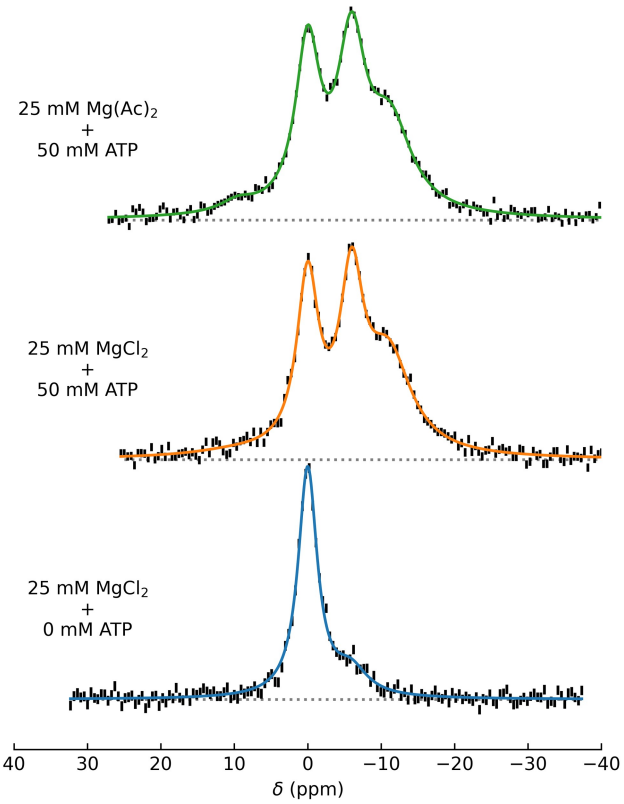

Figure 1. ^{31}Mg β-NMR spectra in EMIM-Ac with different amounts of solutes ($MgCl_2$, $Mg(Ac)_2$, and ATP), recorded at 295 K and 3.20 T (≈43.1 MHz). The striking differences in the spectra recorded with and without added ATP are a strong indication of Mg^{II}-ATP complexation. The resonance at 0 ppm reflects the binding of Mg^{II} to the solvent anions (used as an in situ reference),[40] the resonance at −6 ppm is assigned to a di-nuclear ^{31}MgMg-ATP species, and the broad resonance at approximately −11 ppm is assigned to ^{31}Mg-ATP. The vertical scale is the same for all spectra. Each data point is drawn as a vertical black line, denoting the span of the (statistical) error bars. The solid coloured lines represent fits to a sum of Lorentzians[40] and the baselines are indicated by dotted grey lines.

Next, a series of ^{31}Mg β-NMR experiments were conducted in solutions with 50 mM ATP and 25 mM of either $MgCl_2$ or $Mg(Ac)_2{\cdot}4H_2O$ (see Figure 1). It is evident that the spectra recorded in the presence and absence of ATP differ significantly, providing a strong indication for ^{31}Mg binding to ATP. Note that the spectra recorded using different Mg^{II} salts are essentially identical, implying that the anion of the Mg-salt does not affect the spectroscopic signature—further evidence of complexation by our probe. In the presence of ATP, three main peaks are easily distinguishable. These can be quantified by fitting to a sum of Lorentzians and a baseline,[40,48] identifying unique coordination environments at: 0 ppm (from the solvent), −6 ppm, and −11 ppm. To place an assignment on the remaining peaks, we consider their evolution with solute concentration, in conjunction with the species present in solution at equilibrium.[40]

Analogous to the behaviour in aqueous solution, we expect Mg^{II} to form both mono- and di-nuclear species when binding to ATP in EMIM-Ac (see e.g., ref. [49,52]). Consequently, we anticipate the presence of the following species in solution prior to introducing any ^{31}Mg: Mg^{II}, ATP, Mg-ATP, and Mg_2-ATP. The persistence of the "solvent" peak at all solute concentrations (see below) suggests that the binding of ^{31}Mg is "staged", with the implanted ^{31}Mg initially forming complexes with the solvent acetate anions. This is reasonable, given their significant abundance (≈6 M). Subsequently, upon encounter, the solvent-bound ^{31}Mg may bind to either ATP or Mg-ATP, forming ^{31}Mg-ATP or ^{31}MgMg-ATP, respectively. Any binding to Mg_2-ATP is, presumably, negligible. Thus, our focus in the following is on the presence of ATP and Mg-ATP, which are disposed to form complexes with the implanted ^{31}Mg.

^{31}Mg β-NMR spectra recorded at different $MgCl_2$ concentrations (0 mM to 200 mM) with a constant ATP concentration (50 mM) are shown in Figure 2. Under these conditions, the main species present in solution prior to ^{31}Mg implantation are controlled by the amount of added $MgCl_2$. At high concentration (≥100 mM), all ATP are saturated by the "carrier" Mg^{II} (i.e., essentially only Mg-ATP is present as a potential ligand for the implanted ^{31}Mg), as confirmed by ^{31}P NMR.[40] The ^{31}Mg β-NMR spectra at these conditions, apart from the solvent peak, show only one additional resonance at −6 ppm, suggesting it corresponds to the di-nuclear complex. We therefore assign this signal to ^{31}MgMg-ATP. As the $MgCl_2$ concentration is decreased to ≤50 mM, the amplitude of the −6 ppm peak decreases systematically, coinciding with the emergence and growth of a signal at −11 ppm. At these conditions, the solutions contain both free and Mg-bound ATP, with their respective populations increasing (decreasing) as the $MgCl_2$ concentration is lowered.[40] This consistency implies that the −11 ppm signal

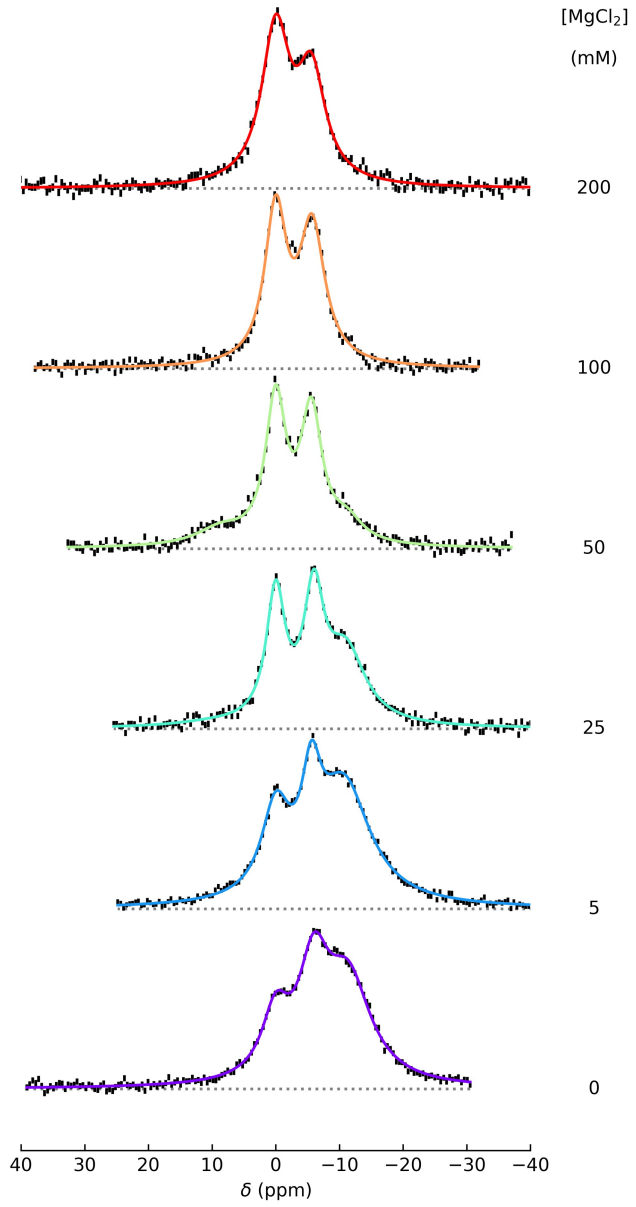

Figure 2. ^{31}Mg β-NMR spectra in EMIM-Ac at various $MgCl_2$ concentrations (indicated in the inset) and 50 mM ATP, recorded at 295 K and 3.20 T (≈43.1 MHz). The resonance at 0 ppm reflects the binding of Mg^{II} to the solvent anions (used as an in situ reference),[40] the resonance at −6 ppm is assigned to a di-nuclear ^{31}MgMg-ATP species, and the broad resonance at approximately −11 ppm is assigned to ^{31}Mg-ATP. The vertical scale is the same for all spectra. Each data point is drawn as a vertical black line, denoting the span of the (statistical) error bars. The solid lines represent a fit to a sum of Lorentzians[40] and the baselines are indicated by dotted grey lines.

is due to the formation of a mono-nuclear complex and we assign it to ^{31}Mg-ATP. Note that measurements using instead $Mg(Ac)_2{\cdot}4H_2O$ as the "carrier" salt yielded identical results.[40] Similarly, spectra recorded using ATP as the "titrant" (at fixed $MgCl_2$ concentration) were also found to be consistent with the above interpretation (i.e., the −6 ppm peak grows with increasing ATP concentration).[40] Together, these observations confirm that the observed behaviour for implanted ^{31}Mg is intrinsic.

With the major features of Figure 2 outlined above, we consider some of the spectral details further. First, we note that the main feature of the resonance at −11 ppm, assigned to ^{31}Mg-ATP, is its relatively large linewidth.[40] This observation is consistent with several possible binding modes of Mg^{II} to ATP.[53–55] Accompanying the appearance of this signal is a noticeable drop in intensity of the "solvent" peak, particularly when the $MgCl_2$ concentration is ≤25 mM. This may indicate that the binding of $^{31}Mg^{II}$ to free ATP is faster than to Mg-ATP, resulting in quicker depopulation of the solvent-bound complex.[56] At all other conditions, the amplitude of the 0 ppm resonance is maximal, indicating that all ^{31}Mg nuclei occupy this structure (for at least ≈1 ms[57]) during the 1s RF pulse. In contrast, our ^{31}P NMR data[40] demonstrate that, at equilibrium, the Mg^{II} binding to ATP is shifted significantly towards the Mg-ATP complex. From this we conclude that the ^{31}Mg β-NMR spectra reflect a non-equilibrium situation, wherein the implanted ^{31}Mg remain complexed with the solvent acetate anions initially (for at least ≈1 ms) after implantation and subsequently form an ATP-containing complex during the (rather long) RF pulse. This interpretation is supported by the fact that neither of the ^{31}Mg ATP or ^{31}MgMg-ATP resonance amplitudes reach their maximum, though both scale according to the ratio of added ATP and Mg^{II} concentrations, which determines the abundance of ATP and Mg-ATP in solution. Moreover, as alluded above, the sum over all resonance amplitudes always exceeds the spectrum's "baseline",[40] meaning that the observed coordination species undergo dynamic exchange during the measurement's time window, supporting the interpretation of "staged" binding. In the future, it would be interesting to follow this process directly (e.g., using spectral hole-burning[58]).

A surprising result from Figure 2 is in the experiment with only trace amounts of implanted ^{31}Mg (i.e., no added $MgCl_2$). Here, only the mono-nuclear complex was expected to form, but the spectrum also showed a minor peak at −6 ppm, implying the formation of ^{31}MgMg-ATP. This is likely due to the presence of a small amount of Mg^{II} (i.e., as an impurity) in either the commercial ATP salt (estimated to be 18(1) μM from inductively coupled plasma mass spectrometry (ICP-MS) measurements[40]) or the solvent (up to ≈1 mM[16]).

At the high $MgCl_2$ concentration limit, an increase from 100 mM to 200 mM gives rise to a drop in the intensity of the −6 ppm signal. Based on the ^{31}P NMR data and the derived equilibrium constants for the formation of Mg-ATP and Mg_2-ATP,[40] it is predicted that the concentration of Mg-ATP is decreased in the sample with 200 mM $MgCl_2$, due to a shift in the equilibrium towards Mg_2-ATP. This is expected to also give rise to a decrease in ^{31}MgMg-ATP signal, in agreement with the observed trend (see Figure 2), confirming the interpretation of the β-NMR data.

Thus far, we have not discussed the impact of any H_2O present in our solutions. H_2O is a common impurity in hygroscopic RTILs such as EMIM-Ac[59] and we previously

considered it as an explanation for the "minor" solvent peak near −6 ppm[16] (see Figure 1); however, a subsequent measurement with intentionally added water rules this out,[40] eliminating it as a possible "contaminant" for the peak assigned to ^{31}Mg-ATP. Another important consideration is how H_2O content influences the pH of our solutions, which is well-known to affect the complexation of Mg^{II} and ATP in aqueous solution. In pure EMIM-Ac, assuming that no groups exhibit proton dissociation equilibria, the pH of the solution is, by definition, undefined; however, this is not a practical issue as, based on Fourier transform infrared (FTIR) spectroscopy measurements,[40] the water content of "fresh" EMIM-Ac is up to ≈1 % H_2O (v/v), placing our solutions in the extreme basic limit (i.e., pH≈14).[60] This suggests that any Mg^{II} coordination to ATP's nucleobase, known to occur at low pH,[61] is unlikely. Of greater importance though is the possibility of ATP hydrolysis occurring in EMIM-Ac. Our ^{31}P NMR data[40] reveal that a small fraction of ATP is hydrolyzed, producing adenosine 5′-diphosphate (ADP) and inorganic phosphate; however, the measurements indicate that this amount is minor (≈4 % to ≈8 % of the total ATP content).[40] While we cannot completely exclude the possibility that minor signals appear in the ^{31}Mg β-NMR data due to these species, we note that the spectroscopic signature for Mg^{II} binding to ADP differs from ATP.[40]

Finally, to further substantiate the interpretation of the ^{31}Mg β-NMR spectra, we used DFT calculations[62] to determine the optimum coordination geometry and corresponding chemical shielding tensor for the Mg-ATP and Mg_2-ATP complexes.[40] Specifically, starting from analogous structures in aqueous solution,[54] we considered the species $[Mg\text{-}ATP(Ac)_2]^{4-}$ and $[Mg_2\text{-}ATP(Ac)_4]^{4-}$, whose geometries and shieldings were computed using B3LYP/pc-2[64–69] and B3LYP/pcSseg-2,[64–67,70] respectively, each using an integral equation formalism of the polarizable continuum model (IEFPCM)[71,72] to account for the solvent. The fact that the geometry optimizations for these structures converged to energy minima demonstrates that they are stereochemically possible in EMIM-Ac. In all cases, the Mg^{II} were found to be hexacoordinated by oxygen from the phosphate and acetate groups (see Figure 3), the latter being either mono-

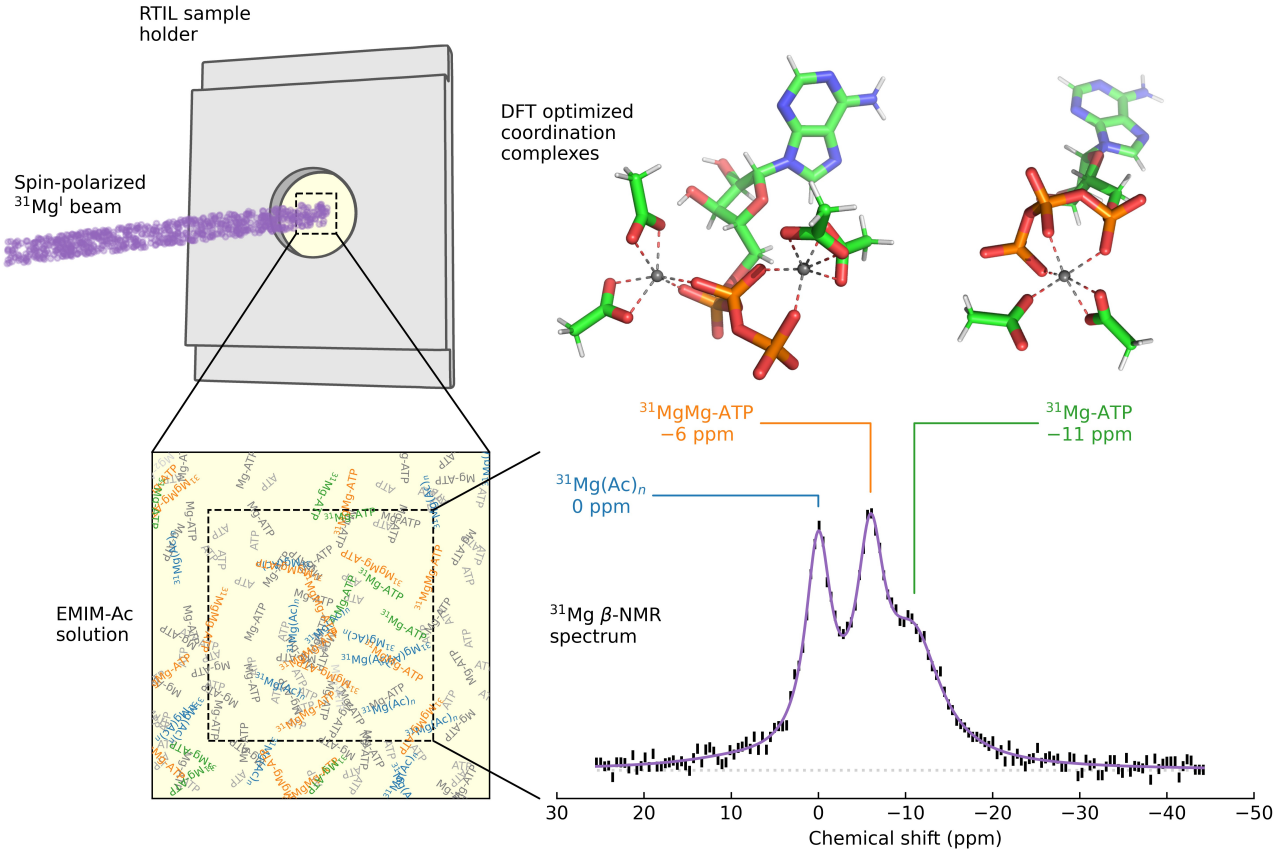

Figure 3. Summary of the ^{31}Mg β-NMR experiments probing Mg^{II} binding to ATP in EMIM-Ac. Nuclear spin-polarized $^{31}Mg^{I}$[42] was implanted into EMIM-Ac solutions suspended vertically within an aluminum alloy plate inside an accelerator beamline under UHV.[16,34,40] During implantation, the probe rapidly oxidizes to $^{31}Mg^{II}$,[16] whereafter it binds (initially) to the solvent acetate anions and subsequently forms ^{31}Mg-ATP or ^{31}MgMg-ATP. The formation of either complex depends chiefly on the amount of free and Mg-complexed ATP present prior to implantation. Using a CW resonance technique,[11,46,47] our β-NMR spectra reveal distinct chemical shifts, whose structural assignments (indicated in the inset) are derived from their systematic evolution with solute concentration. Here, the model spectrum corresponds to the experiment with 50 mM ATP and 25 mM $MgCl_2$ (see Figures 1 and 2). The large resonance amplitudes indicate that all three species undergo dynamic exchange on the millisecond timescale. Structures for the mono- and di-nuclear complexes (obtained from DFT calculations[40,62]) are also shown (drawn using PyMOL[63]).

or bi-dentate (within the first coordination sphere). Note that two configurations for the Mg-ATP complex were found, both containing Mg^{II} coordinated to all three phosphates.[40] It is conceivable that there are other (local) minima on the potential energy surface (i.e., several conformers of the Mg-ATP complex may co-exist at room temperature), in qualitative agreement with the large linewidth of this resonance in our data. Conversely, only a single structure for Mg_2-ATP was found, with one Mg^{II} coordinating to the α- and β-phosphate, and the other to the β- and γ-phosphate. The calculated (isotropic) shieldings for the Mg-ATP (576.4 ppm and 578.8 ppm) and Mg_2-ATP (566.8 ppm and 568.0 ppm) species lead to a chemical shift difference of 8 ppm to 12 ppm.[40] Noting that the computed ^{31}Mg-ATP shift is upfield from ^{31}MgMg-ATP, we obtain reasonable agreement (within the error of the calculations) with the experimental difference of ≈5 ppm, providing additional support for the assignment of the ^{31}Mg β-NMR resonances.

Conclusion

In summary, we have shown the first instance of an ion-implanted β-NMR probe (^{31}Mg) binding to a solute molecule (ATP) before the probe spin depolarizes. This is a necessary prerequisite for the general application of β-NMR spectroscopy in solution chemistry and our result holds promise for future applications in biochemistry. For the case of Mg^{II} binding to ATP in the RTIL EMIM-Ac, we were able to resolve distinct Mg^{II}-ATP coordination environments using the short-lived β-emitter ^{31}Mg. Based on their variation with solute concentration, the recorded resonances have been assigned to: solvent (acetate) bound ^{31}Mg (0 ppm), ^{31}MgMg-ATP (−6 ppm), and ^{31}Mg-ATP (−11 ppm). From the persistence of the "solvent" signal across all measurements, the formation of these species was found to be "staged": the implanted ^{31}Mg initially binds to the solvent, then associates with either ATP or Mg-ATP, depending on their (equilibrium) concentrations in solution. Using DFT calculations, structures for both the mono- and di-nuclear coordination complexes were identified, whose computed isotropic shielding constants were found to be consistent with the measured ^{31}Mg chemical shifts. These findings, along with a sketch of the β-NMR experiments, are illustrated in Figure 3. As a final and important point, the ^{31}Mg β-NMR experiments allow for elucidation of Mg^{II} containing species at extremely low probe concentrations (<1 nM) and under conditions where no other experimental technique can provide useful data.

Acknowledgements

We thank: R. Abasalti, F. Ames, D. J. Arseneau, S. Daviel, B. Hitti, S. Saminathan, B. Smith, and D. Vyas (TRIUMF) for their excellent technical support; V. Lai (Pacific Centre for Isotopic and Geochemical Research) for assistance with the ICP-MS measurements; and C. Lim (Institute of Biomedical Sciences, Academia Sinica) for sharing their optimized geometries of the Mg-ATP complexes (in aqueous solution). L.H. thanks The Danish Council for Independent Research | Natural Sciences, the Agency for Science, Technology and Innovation under the Ministry of Higher Education and Science, Denmark, for financial support. S.J. and R.K.O.S. acknowledge financial support from the SNF and the University of Zurich. R.F.K., W.A.M., and M.S acknowledge financial support from their respective NSERC Discovery grants. Additional support was provided to some of the authors through IsoSiM fellowships (A.C. and R.M.L.M.) and QuEST fellowships (M.H.D., D.F., and V.L.K). TRIUMF receives federal funding via a contribution agreement through the NRC and the NSERC (RGPIN-2018-04030).

Conflict of Interest

The authors declare no conflict of interest.

Data Availability Statement

Additional data that support the findings of this study are available in the Supporting Information of this article. Raw data from the ^{31}Mg β-NMR measurements performed at TRIUMF are publicly available at https://cmms.triumf.ca/ under experiment numbers M1424 and L131.

Keywords: Coordination Modes · Ionic Liquids · Magnesium · NMR Spectroscopy · Nucleosides · Radiochemistry

[1] M. E. Maguire, J. A. Cowan, *BioMetals* **2002**, *15*, 203–210.
[2] C. B. Black, H.-W. Huang, J. A. Cowan, *Coord. Chem. Rev.* **1994**, *1N35–136*, 165–202.
[3] D. R. Case, J. Zubieta, R. P. Doyle, *Molecules* **2020**, *25*, 3172.
[4] E. Freisinger, R. K. O. Sigel, *Chimia* **2019**, *73*, 185–193.
[5] N. J. Stone, Table of Recommended Nuclear Magnetic Dipole Moments: Part I—Long-lived States, INDC(NDS)-0794, International Atomic Energy Agency, Vienna, Austria **2019**.
[6] N. J. Stone, Table of Nuclear Electric Quadrupole Moments, INDC(NDS)-0833, International Atomic Energy Agency, Vienna, Austria **2021**.
[7] J. W. Akitt in *Multinuclear NMR* (Eds.: J. Mason), Springer, Boston, **1987**, chap. 7, pp. 189–220.
[8] J. C. C. Freitas, M. E. Smith in *Annual Reports on NMR Spectroscopy, Vol. 75* (Eds.: G. A. Webb), Academic Press, Oxford, **2012**, chap. 2, pp. 25–114.
[9] C. Ouellet, B. Singh, *Nucl. Data Sheets* **2013**, *114*, 209–396.
[10] H. Ackermann, P. Heitjans, H.-J. Stöckmann, *Topics in Current Physics, Vol. 31* (Eds.: J. Christiansen), Springer, Berlin, **1983**, chap. 6, pp. 291–361.
[11] W. A. MacFarlane, *Solid State Nucl. Magn. Reson.* **2015**, *68–69*, 1–12.
[12] W. A. MacFarlane, *Z. Phys. Chem.* **2022**, *236*, 757–798.
[13] A. J. Pell, G. Pintacuda, C. P. Grey, *Prog. Nucl. Magn. Reson. Spectrosc.* **2019**, *111*, 1–271.
[14] I. McKenzie, M. Harada, R. F. Kiefl, C. D. P. Levy, W. A. MacFarlane, G. D. Morris, S.-I. Ogata, M. R. Pearson, J. Sugiyama, *J. Am. Chem. Soc.* **2014**, *136*, 7833–7836.

[15] R. M. L. McFadden, T. J. Buck, A. Chatzichristos, C.-C. Chen, K. H. Chow, D. L. Cortie, M. H. Dehn, V. L. Karner, D. Koumoulis, C. D. P. Levy, C. Li, I. McKenzie, R. Merkle, G. D. Morris, M. R. Pearson, Z. Salman, D. Samuelis, M. Stachura, J. Xiao, J. Maier, R. F. Kiefl, W. A. MacFarlane, *Chem. Mater.* **2017**, *29*, 10187–10197.

[16] D. Szunyogh, R. M. L. McFadden, V. L. Karner, A. Chatzichristos, T. Day Goodacre, M. H. Dehn, L. Formenti, D. Fujimoto, A. Gottberg, E. Kallenberg, I. Kálomista, R. F. Kiefl, F. H. Larsen, J. Lassen, C. D. P. Levy, R. Li, W. A. MacFarlane, I. McKenzie, G. D. Morris, S. Pallada, M. R. Pearson, S. P. A. Sauer, P. Schaffer, P. W. Thulstrup, L. Hemmingsen, M. Stachura, *Dalton Trans.* **2018**, *47*, 14431–14435.

[17] A. D. Hillier, S. J. Blundell, I. McKenzie, I. Umegaki, L. Shu, J. A. Wright, T. Prokscha, F. Bert, K. Shimomura, A. Berlie, H. Alberto, I. Watanabe, *Nat. Rev. Methods Primers* **2022**, *2*, 4.

[18] I. McKenzie, *Annu. Rep. Prog. Chem. Sect. C* **2013**, *109*, 65–112.

[19] K. Asahi, K. Matsuta, *Nucl. Phys. A* **2001**, *693*, 63–76.

[20] F. H. McGee, I. McKenzie, T. Buck, C. R. Daley, J. A. Forrest, M. Harada, R. F. Kiefl, C. D. P. Levy, G. D. Morris, M. R. Pearson, J. Sugiyama, D. Wang, W. A. MacFarlane, *J. Phys. Conf. Ser.* **2014**, *551*, 012039.

[21] I. McKenzie, C. R. Daley, R. F. Kiefl, C. D. P. Levy, W. A. MacFarlane, G. D. Morris, M. R. Pearson, D. Wang, J. A. Forrest, *Soft Matter* **2015**, *11*, 1755–1761.

[22] I. McKenzie, Y. Chai, D. L. Cortie, J. A. Forrest, D. Fujimoto, V. L. Karner, R. F. Kiefl, C. D. P. Levy, W. A. MacFarlane, R. M. L. McFadden, G. D. Morris, M. R. Pearson, S. Zhu, *Soft Matter* **2018**, *14*, 7324–7334.

[23] I. McKenzie, D. Fujimoto, V. L. Karner, R. Li, W. A. MacFarlane, R. M. L. McFadden, G. D. Morris, M. R. Pearson, A. N. Raegen, M. Stachura, J. O. Ticknor, J. A. Forrest, *J. Chem. Phys.* **2022**, *156*, 084903.

[24] V. L. Karner, T. Liu, I. Mckenzie, A. Chatzichristos, D. L. Cortie, G. D. Morris, R. F. Kiefl, R. M. L. Mcfadden, Z. Fakhraai, M. Stachura, W. A. Macfarlane, *JPS Conf. Proc.* **2018**, *21*, 011022.

[25] D. Fujimoto, R. M. L. McFadden, M. H. Dehn, Y. Petel, A. Chatzichristos, L. Hemmingsen, V. L. Karner, R. F. Kiefl, C. D. P. Levy, I. McKenzie, C. A. Michal, G. D. Morris, M. R. Pearson, D. Szunyogh, J. O. Ticknor, M. Stachura, W. A. MacFarlane, *Chem. Mater.* **2019**, *31*, 9346–9353.

[26] A. Gottberg, M. Stachura, M. Kowalska, M. L. Bissell, V. Arcisauskaite, K. Blaum, A. Helmke, K. Johnston, K. Kreim, F. H. Larsen, R. Neugart, G. Neyens, R. F. Garcia Ruiz, D. Szunyogh, P. W. Thulstrup, D. T. Yordanov, L. Hemmingsen, *ChemPhysChem* **2014**, *15*, 3929–3932.

[27] T. Sugihara, M. Mihara, J. Shimaya, K. Matsuta, M. Fukuda, J. Ohno, M. Tanaka, S. Yamaoka, K. Watanabe, S. Iwakiri, R. Yanagihara, Y. Tanaka, H. Du, K. Onishi, S. Kambayashi, T. Minamisono, D. Nishimura, T. Izumikawa, A. Ozawa, Y. Ishibashi, A. Kitagawa, S. Sato, M. Torikoshi, S. Momota, *Hyperfine Interact.* **2017**, *238*, 20.

[28] M. Mihara, T. Sugihara, M. Fukuda, A. Homma, T. Izumikawa, A. Kitagawa, K. Matsuta, T. Minaisono, S. Momota, T. Nagatomo, H. Nishibata, D. Nishimura, K. Ohnishi, T. Ohtsubo, A. Ozawa, S. Sato, M. Tanaka, R. Wakabayashi, S. Yagi, R. Yanagihara, *Hyperfine Interact.* **2019**, *240*, 113.

[29] R. D. Harding, S. Pallada, J. Croese, A. Antušek, M. Baranowski, M. L. Bissell, L. Cerato, K. M. Dziubinska-Kühn, W. Gins, F. P. Gustafsson, A. Javaji, R. B. Jolivet, A. Kanellakopoulos, B. Karg, M. Kempka, V. Kocman, M. Kozak, K. Kulesz, M. M. Flores, G. Neyens, R. Pietrzyk, J. Plavec, M. Pomorski, A. Skrzypczak, P. Wagenknecht, F. Wienholtz, J. Wolak, Z. Xu, D. Zakoucky, M. Kowalska, *Phys. Rev. X* **2020**, *10*, 041061.

[30] J. Croese, M. Baranowski, M. L. Bissell, K. M. Dziubinska-Kühn, W. Gins, R. D. Harding, R. B. Jolivet, A. Kanellakopoulos, B. Karg, K. Kulesz, M. Madurga Flores, G. Neyens, S. Pallada, R. Pietrzyk, M. Pomorski, P. Wagenknecht, D. Zakoucky, M. Kowalska, *Nucl. Instrum. Methods Phys. Res. Sect. A* **2021**, *1020*, 165862.

[31] M. Mihara, Y. Otani, Y. Kimura, R. Wakabayashi, N. Noguchi, M. Ogose, T. Izumikawa, H. Takahashi, M. Sato, K. Takatsu, G. Takayama, S. Momota, H. Okumura, M. Fukuda, M. Fukutome, D. Nishimura, K. Matsuta, T. Minamisono, T. Ohtsubo, A. Ozawa, T. Nagatomo, A. Kitagawa, S. Sato, *Hyperfine Interact.* **2021**, *242*, 49.

[32] Note that experiments in liquids are technically challenging due to, in part, the vacuum requirements of the accelerator beamlines used to deliver the β-NMR probes.

[33] In the remainder of the text, all radioactive magnesium is explicitly labelled as ^{31}Mg. The absence of any specific isotopic identifier (e.g., Mg or Mg^{II}) denotes non-radioactive magnesium (in their natural isotopic abundances).

[34] R. M. L. McFadden, A. Chatzichristos, M. H. Dehn, D. Fujimoto, H. Funakubo, A. Gottberg, T. Hitosugi, V. L. Karner, R. F. Kiefl, M. Kurokawa, J. Lassen, C. D. P. Levy, R. Li, G. D. Morris, M. R. Pearson, S. Shiraki, M. Stachura, J. Sugiyama, D. M. Szunyogh, W. A. MacFarlane, *JPS Conf. Proc.* **2018**, *21*, 011047.

[35] F. H. Westheimer, *Science* **1987**, *235*, 1173–1178.

[36] S. C. L. Kamerlin, P. K. Sharma, R. B. Prasad, A. Warshel, *Q. Rev. Biophys.* **2013**, *46*, 1–132.

[37] L. S. Koehler, F. Jarnagm, R. G. Hiskey, L. G. Pedersen, K. A. Koehler, *J. Inorg. Biochem.* **1987**, *29*, 153–164.

[38] I. Bertini, H. B. Gray, E. I. Stiefel, J. S. Valentine, *Biological Inorganic Chemistry: Structure and Reactivity*, University Science Books, Sausalito, USA **2007**.

[39] The EMIM-Ac dielectric constant is estimated to be ≈13, based on an empirical model accounting for its structure.[73]

[40] See the Supporting Information of this article for details.

[41] C. D. P. Levy, M. R. Pearson, R. F. Kiefl, E. Mané, G. D. Morris, A. Voss, *Hyperfine Interact.* **2014**, *225*, 165–172.

[42] C. D. P. Levy, M. R. Pearson, M. H. Dehn, V. L. Karner, R. F. Kiefl, J. Lassen, R. Li, W. A. MacFarlane, R. M. L. McFadden, G. D. Morris, M. Stachura, A. Teigelhöfer, A. Voss, *Hyperfine Interact.* **2016**, *237*, 162.

[43] E. F. Smith, I. J. Villar Garcia, D. Briggs, P. Licence, *Chem. Commun.* **2005**, 5633–5635.

[44] A. Nazet, S. Sokolov, T. Sonnleitner, T. Makino, M. Kanakubo, R. Buchner, *J. Chem. Eng. Data* **2015**, *60*, 2400–2411.

[45] G. D. Morris, *Hyperfine Interact.* **2014**, *225*, 173–182.

[46] M. Newton, E. Breeds, R. Morris, *Electronics* **2017**, *6*, 89.

[47] S. R. Kreitzman, *Hyperfine Interact.* **1991**, *65*, 1055–1069.

[48] D. Fujimoto, *J. Open Source Software* **2021**, *6*, 3598.

[49] A. C. Storer, A. Cornish-Bowden, *Biochem. J.* **1976**, *159*, 1–5.

[50] E. O. Bishop, S. J. Kimber, D. Orchard, B. E. Smith, *Biochim. Biophys. Acta Bioenerg.* **1981**, *635*, 63–72.

[51] T. Glonek, *Int. J. Biochem.* **1992**, *24*, 1533–1559.

[52] S. Nakamura, S. Koga, N. Shibuya, K. Seo, S. Kidokoro, *Thermochim. Acta* **2013**, *563*, 82–89.

[53] H. Sigel, R. Griesser, *Chem. Soc. Rev.* **2005**, *34*, 875–900.

[54] T. Dudev, C. Grauffel, C. Lim, *Sci. Rep.* **2017**, *7*, 42377.

[55] F. P. Buelens, H. Leonov, B. L. de Groot, H. Grubmüller, *J. Chem. Theory Comput.* **2021**, *17*, 1922–1930.

[56] The apparent growth of the "solvent" peak with increasing $[MgCl_2]$ in Figure 2 likely reflects the shift in both binding competition and "site" availability as ATP becomes progressively saturated by the added Mg^{II}. That is, as the concen-

trations of "free" ATP and Mg ATP decrease, so too does the rate of de-population for the solvent-bound complex.
[57] The ≈1 ms timescale refers to the minimum residence time required for sufficient depolarization by the RF field to produce resonance amplitudes compatible with our observations. This value can be inferred from simulations of the β-NMR lineshape (see e.g., ref. [74]).
[58] P. L. Kuhns, M. S. Conradi, *J. Chem. Phys.* **1982**, *77*, 1771–1778.
[59] We note that some H_2O is introduced in our solutions through the addition of the ATP and $Mg(Ac)_2$ salts.[40]
[60] C. A. Ober, R. B. Gupta, *Ind. Eng. Chem. Res.* **2012**, *51*, 2524–2530.
[61] L. Jiang, X.-A. Mao, *Spectrochim. Acta Part A* **2001**, *57*, 1711–1716.
[62] Gaussian 16 (Revision C.01), M. J. Frisch, G. W. Trucks, H. B. Schlegel, G. E. Scuseria, M. A. Robb, J. R. Cheeseman, G. Scalmani, V. Barone, G. A. Petersson, H. Nakatsuji, X. Li, M. Caricato, A. V. Marenich, J. Bloino, B. G. Janesko, R. Gomperts, B. Mennucci, H. P. Hratchian, J. V. Ortiz, A. F. Izmaylov, J. L. Sonnenberg, D. Williams-Young, F. Ding, F. Lipparini, F. Egidi, J. Goings, B. Peng, A. Petrone, T. Henderson, D. Ranasinghe, V. G. Zakrzewski, J. Gao, N. Rega, G. Zheng, W. Liang, M. Hada, M. Ehara, K. Toyota, R. Fukuda, J. Hasegawa, M. Ishida, T. Nakajima, Y. Honda, O. Kitao, H. Nakai, T. Vreven, K. Throssell, J. A. Montgomery, Jr., J. E. Peralta, F. Ogliaro, M. J. Bearpark, J. J. Heyd, E. N. Brothers, K. N. Kudin, V. N. Staroverov, T. A. Keith, R. Kobayashi, J. Normand, K. Raghavachari, A. P. Rendell, J. C. Burant, S. S. Iyengar, J. Tomasi, M. Cossi, J. M. Millam, M. Klene, C. Adamo, R. Cammi, J. W. Ochterski, R. L. Martin, K. Morokuma, O. Farkas, J. B. Foresman, and D. J. Fox, Gaussian Inc., Wallingford (USA), **2016**.
[63] The PyMOL molecular graphics system, Schrödinger, LLC, New York (USA), **2021**.
[64] A. D. Becke, *Phys. Rev. A* **1988**, *38*, 3098–3100.
[65] C. Lee, W. Yang, R. G. Parr, *Phys. Rev. B* **1988**, *37*, 785–789.
[66] A. D. Becke, *J. Chem. Phys.* **1993**, *98*, 5648–5652.
[67] P. J. Stephens, F. J. Devlin, C. F. Chabalowski, M. J. Frisch, *J. Phys. Chem.* **1994**, *98*, 11623–11627.
[68] F. Jensen, *J. Chem. Phys.* **2001**, *115*, 9113–9125.
[69] F. Jensen, *J. Phys. Chem. A* **2007**, *111*, 11198–11204.
[70] F. Jensen, *J. Chem. Theory Comput.* **2015**, *11*, 132–138.
[71] J. Tomasi, B. Mennucci, E. Cancès, *J. Mol. Struct.* **1999**, *464*, 211–226.
[72] J. Tomasi, B. Mennucci, R. Cammi, *Chem. Rev.* **2005**, *105*, 2999–3094.
[73] Y. Zhou, Z. Lin, K. Wu, G. Xu, C. He, *Chin. J. Chem. Eng.* **2014**, *22*, 79–88.
[74] D. J. Fujimoto, PhD thesis, University of British Columbia (Canada), **2021**.

Manuscript received: May 16, 2022
Accepted manuscript online: June 19, 2022
Version of record online: July 14, 2022